JTCM Journal of Traditional Chinese Medicine

Online Submissions: http://www.journaltcm.com
ISSN 0255-2922
info@journaltcm.com

Research Article

Effect of moxibustion on autophagy and the inflammatory response of synovial cells in rheumatoid arthritis model rats

HAO Feng, WANG Qiang, LIU Lei, WU Libin, CAI Ronglin, SANG Jiajia, HU Jun, WANG Jie, YU Qing, HE Lu, SHEN Yingchao, MIAO Yiming, HU Ling, WU Zijian

HAO Feng, College of Acupuncture-moxibustion and Tuina, Nanjing University of Chinese Medicine, Nanjing 210023, China; Translational Medicine Research Center of Nanjing University of Chinese Medicine, Nanjing 210023, China
WANG Qiang, Changshu Hospital Affiliated to Nanjing University of Chinese Medicine, Changshu 215500, China
LIU Lei, WU Libin, College of Acupuncture-moxibustion and Tuina, Anhui University of Chinese Medicine, Hefei 230012, China
CAI Ronglin, WANG Jie, YU Qing, HE Lu, HU Ling, WU Zijian, College of Acupuncture-moxibustion and Tuina, Anhui University of Chinese Medicine, Hefei 230012, China; Institute of Acupuncture and Meridian, Anhui Academy of Chinese Medicine, Hefei 230038, China
SANG Jiajia, Affiliate Hospital of Nanjing University of Chinese Medicine/Jiangsu Province of Chinese Medicine, Nanjing 210029, China
HU Jun, the first clinical medical college of Nanjing University of Chinese Medicine, Nanjing 210029, China
SHEN Yingchao, MIAO Yiming, Changshu Hospital Affiliated to Nanjing University of Chinese Medicine, Changshu 215500, China
Supported by the University Natural Science Research Program of Jiangsu: Study on the Mechanism Of Moxibustion Regulating Autophagy in RA synovial Fibroblasts Based on PI3K/Akt/mTOR Pathway (No. 18KJB360005), the 973 Program of China: Effect and Biological Mechanism of Heat, Light and Smoking in Moxibustion (No. 2015CB554504), and funded by the Priority Academic Program Development of Jiangsu Higher Education Institutions (Integration of Chinese and Western Medicine), the Exploration and Scientific Research Project of Anhui University of Chinese Medicine: Clinical Application and Mechanism Study of Moxibustion (No. 2016ts024)
Correspondence to: WU Zijian, HU Ling, College of Acupuncture-moxibustion and Tuina, Anhui University of Chinese Medicine, Hefei, 230012, China; Institute of Acupuncture and Meridian, Anhui Academy of Chinese Medicine, Hefei, 230038, China. wuzijian@ahtcm.edu.cn; hulingtcm@126.com
Telephone: +86-15156096557; +86-13956933188
DOI: 10.19852/j.cnki.jtcm.20210324.002
Received: November 21, 2020
Accepted: February 16, 2021
Available online: March 24, 2021

Abstract

OBJECTIVE: To investigate the effect of moxibustion on synovitis and the autophagy of synoviocytes in rheumatoid arthritis (RA).

METHODS: Forty Sprague-Dawley rats were randomly divided into a normal group, model group, moxibustion group, cigarette moxibustion group, and medicine group, with eight rats included in each group. The RA model was established by subcutaneous injection of complete Freund's adjuvant into the left posterior toe. Rats in the model group were not interfered with. In the moxibustion group, rats were treated by moxibustion, where a 1-cm diameter moxa stick was applied at the left Zusanli (ST 36) point. The distance of the moxa stick to the skin was 2 cm and moxibustion was completed for 20 min daily for 15 d total. In the cigarette moxibustion group, the moxa stick was replaced by a common cigarette. In the medicine group, rats were treated with a tripterygium glycoside suspension (8 mg/kg) once a day for 15 d total. In each group, the left hind limb toe volume was measured with a toe volume meter; the synovial cells were observed by hematoxylin and eosin staining; the interleukin (IL)-4, IL-6, IL-10, IL-1β, IL-23, IL-17, and tumor necrosis factor (TNF)-α levels in serum were measured by enzyme-linked immunosorbent assay; the erythrocyte sedimentation rate (ESR) were detected by Westergren sedimentation rate testing; the C-reactive protein (CRP) and rheumatoid factor (RF) levels in serum were detected by rate nephelometry; the expression levels of ULK1, autophagy-associated protein (Atg)3, Atg5, and Atg12 messenger RNA (mRNA) in synovium were detected by real time-quantitative polymerase chain reaction (RT-qPCR); and the protein expression levels of phosphatidylinositol-3-kinase (PI3K), protein kinase B (Akt), mammalian target of rapamycin (mTOR), LC3-Ⅱ, beclin-1, phosphorylated-PI3K (p-PI3K), p-Akt, p-mTOR in synovium were detected by Western blotting.

RESULTS: Among the RA model rats, joint swelling, an inflammatory reaction, and the proliferation of synovial tissue were obvious and the signal of the PI3K/Akt/mTOR pathway was active, while autophagy was inhibited. Moxibustion at Zusanli (ST36) or intragastric administration of Tripterygium wilfordii glycosides could alleviate the inflammatory reaction of RA rats; relieve the swelling of the toes; downregulate the levels of ESR, CRF, RF; lower the levels of IL-6, IL-1β, TNF-α, and IL-17; and increase the IL-4 and IL-10. At the same time, the mRNA expression levels of ULK1, Atg3, Atg5, and Atg12 and those of LC3-Ⅱ and beclin-1 were increased, while the PI3K, Akt, mTOR, p-PI3K, p-Akt, p-mTOR were decreased. Cigarette moxibustion did not significantly reduce the swelling of the toe joint in RA rats, and was not as good as that of moxibustion or Tripterygium

wilfordii polyglycosides in the effects of inflammation relief and the influences of the levels of ESR, CRF, RF. While cigarette moxibustion has a weak effect to affect the expression of corresponding molecules in autophages and the expression level of the autophagy biomaker in synovial tissue. Moxibustion and tripterygium glycosides can significantly reduce the joint swelling, relieve synovitis and synovial hyperplasia, and inhibit the PI3K/Akt/mTOR signaling pathway to increase autophagy in a manner superior to cigarette moxibustion.

CONCLUSION: Moxibustion can limit the proliferation of synoviocytes in RA rats by inhibiting the PI3K/Akt/mTOR signaling pathway, promoting autophagy, effectively reducing synovitis, and alleviating joint swelling.

Keywords：moxibustion; arthritis, rheumatoid; synovitis; autophagy

1. INTRODUCTION

Rheumatoid arthritis (RA) is a chronic autoimmune disease that is often accompanied by joint deformities, joint pain, and dysfunction.[1] To date, the pathogenesis of RA remains complicated and unclear. At present, it is considered that cellular and humoral immunity dysfunction, synovial inflammation, and pannus hyperplasia are closely related with the development of RA. Long-term use of common clinical medications such as nonsteroidal anti-inflammatory drugs, may lead to gastrointestinal tract stimulation, bone cortical thinning, and other adverse reactions. Moxibustion, as one of the commonly adopted techniques in traditional Chinese medicine, is effective and widely used for treating RA as it is able to repair inflammatory injury, relieve pain, and significantly improve the symptoms and signs of patients.[2, 3]

Recent studies suggest that the abnormal proliferation of synoviocytes plays an important role in the pathogenesis of RA, a process that is closely related to changes in the autophagy pathway of synoviocytes.[4] Some studies found that the autophagic phosphatidylinositol-3-kinase (PI3K) PI3K/Akt/mammalian target of rapamycin (mTOR) pathway of synoviocytes is closely related with RA,[5,6] while other research indicates there are complex feedback mechanisms present between the PI3K/Akt/mTOR signaling pathway and inflammatory cytokines.[7] Moxibustion can effectively promote the apoptosis process of synoviocytes, inhibit the abnormal proliferation of synoviocytes, and repair the morphological structure of synoviocytes.[8] Therefore, regulating the autophagy of synoviocytes may be one of the key mechanisms in moxibustion therapy for RA. At present, however, few studies on the autophagy of moxibustion treatment of RA exist. In this study, an RA rat model was established and moxibustion of the left Zhusanli (ST36) point was used to treat the animals, with a comparison made against the effects of cigarette moxibustion and intragastric administration of tripterygium glycosides. Herein, we sought to discuss the effect of moxibustion, explore the mechanism of moxibustion in treating RA, and provide experimental support for clinical application.

2. MATERIALS AND METHODS

2.1. Animal grouping and model replication and evaluation

Forty male healthy Sprague-Dawley rats with a body weight of (180 ± 20) g were purchased from Shandong Experimental Animal Center in Jinan, China [permit no. SCXK (Lu) 20190003]. After one week of adaptive feeding, the rats were randomly divided into a normal group, model group, moxibustion group, cigarette moxibustion group, and medicine group, 8 in each group. The temperature in the laboratory was (27.0 ± 0.5) ℃, the humidity was 55.5%, and the environment alternated between light and dark every 12 h. All experimental procedures were conducted in strict accordance with the relevant provisions of the guidelines for the good treatment of experimental animals issued by the Ministry of Science and Technology of the People's Republic of China in 2006, making every effort to alleviate the suffering of the animal test subjects.

Our previous study had proven that cold wind and a humid environment combined with the subcutaneous injection of complete Freund's adjuvant (CFA) could successfully establish an RA model.[9–11] In this study, we adopted the same methods. Except in the normal group, all rats were placed into a self-manufactured box in which the humidity was controlled to 80% to 90% by an ultrasonic atomizer, ice was placed to keep the temperature at (6 ± 2) ℃, and an electrical fan was used at the highest level to 12 h a day (20: 00-8: 00) for 20 d total. On the 21st day, the rats were disinfected with 75% alcohol (0180521, Shanghai Suyi Chemical Reagent Co., Ltd., Shanghai, China) on the left hind metatarsus, and 0.15 mL/rat of CFA was injected (SLBW7430; Sigma-Aldrich, St. Louis, MO, USA). During continuous observation for three days, acute inflammation and swelling of the ankle appeared at 24 h and secondary systemic polyarthritis appeared at 48 h relative to the forelimb or contralateral limb, which indicated that the model was established successfully.

2.2. RA intervention

The rats in the normal and model group were captured and fixed on the special hanging wooden frame without any other intervention for 20 min daily for 15 d. In the moxibustion group, the rats were treated with a 1-cm diameter moxa stick (20180704, Nanyang Hanyi AI Rong Co., Ltd., Nanyang, China) at 2 cm away from the acupoint of Zhusanli (ST36). In the cigarette moxibustion group, the moxa stick was replaced by a common cigarette (Anhui Zhongyan Industry Co., Ltd., Hefei, China), the distance and acupoint of moxibustion

are the same as those of moxibustion group. Select acupoints according to the *Acupoint Atlas of Rats in experimental moxibustion*.[12] In the medicine group, the rats were given a tripterygium glycoside suspension (8 mg/kg) (190302; Shanghai Fudan Forward Company, Shanghai, China) and fixed on the special wooden frame for 20 min after gavage daily for 15 d.

2.3. Westergren assay of ESR

Rats were anesthetized with 20% urethane solution (3 mL/kg) (20190213, Shanpu Chemical Co., Ltd., Shanghai, China) intraperitoneally on the next day after the last intervention. Take out the blood and keep in an anticoagulant tube, then transfer the blood into standard Westergren tube. Adjust scale to "0". The Westergren tube was placed strictly vertically at room temperature and avoid sunlight, vibration and blood overflow. One hour later, the distance (mm), which was read out by the automatic ESR instrument (DIESSE, Ves-Matic® 20, Italy), between the bottom of the plasma concave surface and the top of the settling erythrocyte column is the value of ESR.

2.4. Rate nephelometry assay of CRP, RF

Rats in each group were anesthetized with 20% urethane solution (3 mL/kg) (20190213, Shanpu Chemical Co., Ltd., Shanghai, China) intraperitoneally on the next day after the last intervention. We collected abdominal aortic blood and isolated serum by centrifuge (4 ℃, 3000 r/min, 10 min). Then extracted 200 μL serum, and added 50 μL test solution into it as a sample. We transferred the sample to the double light diameter automatic protein analyzer (Beckman Coulter, Immage®, CA, USA). After the detection period (30 s), the contents of CRP and RF were read out.

2.5. RNA and protein analyses

Take 100 mg of synovial tissue from the left hind limb of the toe joint of the rat, and grind it with liquid nitrogen. Total RNA was isolated using Trizol reagent (204403; Life Technologies, Carlsbad, CA, USA). We used the RevertAid™ first Strand cDNA Synthesis Kit (00691399; Thermo Fisher Scientific, Waltham, MA, USA) to execute reverse transcription. RNA concentrations were determined by a Qubit bioanalyzer (QUBIT 2.0, Q32866; Invitrogen, Carlsbad, CA, USA) prior to real-time polymerase chain reaction (PCR) for gene expression. Real-time PCR was accomplished using Novostart® SYBR qPCR SuperMix Plus (novoprotein, 0512841). The reaction conditions were: 95 ℃ for 1 min; 95 ℃ for 20 s, 40 cycles; 60 ℃ for 1 min, 40 cycles. The primers for each detection index were listed in Table 1. The primers of each target gene were provided by Anhui Xin Le Biotechnology Company (Hefei, China). The relative messenger RNA (mRNA) expression was calculated by $2^{-\Delta\Delta Ct}$.

Synovium was taken from the left hind limb joints of the rats and 100 mg was cut up in a homogenizer; in addition, a cracking solution containing Phenyl methyl sulfonyl fluoride (PMSF) (20190315, Solarbio Science & Technology Co., Ltd., Beijing, China) was added to the homogenate, with subsequent placement on ice, and the composition was repeatedly ground several times to ensure the tissues were as crushed as possible. After 30 min of pyrolysis, we performed 13 000 ×g of centrifugation at 4 ℃ for 10 min, extract supernatant, added the buffer solution of the upper sample in a 3∶1 volume, and followed the Western blotting protocol step by step. The antibodies what were used contain: Anti-phosphatidylinositol-3-kinase (PI3K) antibody (GR199664-6, abcam, Cambridge, UK), anti-phosphorylated phosphatidylinositol-3-kinase (p-PI3K) antibody (GR305773-2, abcam, Cambridge, UK), anti-protein kinase B (AKT) antibody (28, Cell Signaling Technology, MA, USA), anti-phosphorylated protein kinase B (p-AKT) antibody (25, Cell Signaling Technology, MA, USA), anti-mammalian target of rapamycin (mTOR) antibody (13J03119451, BIOSS, Beijing, China), anti-phosphorylated mammalian target of rapamycin (p-mTOR) antibody (2, Cell Signaling Technology, MA, USA), anti-microtubule-associated protein light chain 3-II (LC3-II) antibody (13, Cell Signaling Technology, MA, USA), anti-Beclin-1 antibody (GR13053-7, abcam, Cambridge, UK), goat anti-mouse IgG (140193, Zsbio, Beijing, China), goat anti-rabbit IgG (202700514, Zsbio, Beijing, China).

2.6. Hematoxylin and eosin staining

After the last intervention, the rats were anesthetized with 3 mL/kg of 20% urethane solution (20190213, Shanghai Shanpu Chemical Co., Ltd, Shanghai, China) intraperitoneally the next day. Several pieces of joint tissue measuring about 0.5 cm in the left hind limb were obtained and fixed in 4% paraformaldehyde for 12 h, paraffin-embedded (EG1150; Leica Camera AG, Wetzlar, Germany), paraffin-sectioned (RM2245; Leica Camera AG, Wetzlar, Germany), and subjected to a 40 to 45 ℃ water bath. After deparaffination and rehydration, the slices were put into hematoxylin (BA-4097) and dyed for about 2 min. After water washing, differentiation, rinsing, and gradient dehydration, the slices were dyed with 0.5% eosin (BA-4099) ethanol

Table 1 Primers of each target gene

Gene	Amplicon	Forward primer	Reverse primer
β-actin	150	CCCATCTATGAGGGTTACGC	TTTAATGTCACGCACGATTTC
Atg12	111	GCCTCGGAGCAGTTGTTTA	ATGTAGGACCAGTTTACCATCAC
Atg5	104	TCCAACGTGCTTTACTCTCTATC	TGTCAGTTACCAGCGTCAAATA
ULk1	126	ACAGCCTGCGCTTCACACTA	TCTGGTCAGCCACCACACTT
Atg3	138	GTGGCAGCTGGAGATCACTT	ACACCGCTTGTAGCATGGAA

Notes: Atg: autophagy-associated protein; ULK1: autophagy-initiating protein kinase.

solution for one to 3 min. After further dehydration, the slices were washed with 95% ethanol to remove the excess red color, then treated with dimethylbenzene for three to five minutes and sealed with neutral gum. At this point, the morphology of the synovium was observed under a microscope (Nikon Ti; Nikon Corp., Tokyo, Japan).

2.7. Enzyme-linked immunosorbent assay (ELISA) of inflammatory factors in serum

The serum was taken from the refrigerator at −20 ℃, melted, and balanced at room temperature for 20 min. Then, to detect the inflammatory factors (Table 3) according to the steps in the kit's instructions (Cusabio, G22018349). The optical density (OD) value of each hole was detected at a wavelength of 450 nm by an enzyme-labeled instrument (SpectraMax® M2e, Molecular Devices, San Jose, CA, USA) after the termination solution was added. ELISA kits what were used contain: rat interleukin-17 ELISA kit (TSB-ZC7CH3T, Elabscience, Houston, USA), rat interleukin-23 ELISA kit (P7LWW28BF6, Elabscience, Houston, USA), rat tumor necrosis factor-α ELISA kit (G22018349, Cusabio, Houston, USA), rat interleukin-1β ELISA kit (I05018350, Cusabio, Houston, USA), rat interleukin-6 ELISA kit (I11018351, Cusabio, Houston, USA), rat interleukin-4 ELISA kit (H30018353, Cusabio, Houston, USA), rat interleukin-10 ELISA kit (I11018354, Cusabio, Houston, USA).

2.8. Statistical analysis

Data were presented as mean ± standard deviation ($\bar{x}$ ± s). Statistical analysis was performed using SPSS 18.0 (IBM Corp., Armonk, NY, USA). A one-way analysis of variance followed by Tukey's honest significant difference test was used for multiple group comparisons. The statistical significance was considered at $P < 0.05$.

3. RESULTS

3.1. Comparison of swelling of the left hind limbs of rats in each group

Relative to the normal group, left hind limb swelling in the model group was significantly higher (1.88 ± 0.19 *vs* 3.23 ± 0.18, $P < 0.01$). Compare with the model group, the degrees of toe swelling in the moxibustion group and the medicine group were significantly reduced (2.46 ± 0.14 *vs* 3.23 ± 0.18, $P < 0.01$; 2.73 ± 0.16 *vs* 3.23 ± 0.18, $P < 0.01$), while that in the cigarette moxibustion group was not significantly decreased (3.01 ± 0.16 *vs* 3.23 ± 0.18, $P > 0.05$). These results suggest that both moxibustion and *Tripterygium wilfordii* polyglycosides can significantly reduce the swelling degree of the joints in RA model rats, with the effect of moxibustion on detumescence being stronger than those of tripterygium glycosides and cigarette moxibustion.

3.2. Comparison of the morphology of the synovium of the left hind limb joints of rats in each group

In the normal group, the lining cells of the synovial membrane were regularly arranged in a single layer, and the surface of the synovial membrane was smooth and orderly without inflammatory infiltration. In the model group, there was significant inflammatory infiltration observed in the synovium, the surface of the synovium was irregular, and the synovium was proliferated and thickened. Inflammatory infiltration and thickening of the synovium in the moxibustion group, cigarette moxibustion group, and medicine group were relieved to different degrees. Improvements in the moxibustion group and medicine group were better than that in the cigarette moxibustion group (Figure 1).

3.3. Comparison of the ESR, CRP, RF levels in serum of rats in each group

When compared with in the normal group, the levels of ESR, CRP, RF of the model group were significantly increased ($P < 0.01$). When compared with in the model group, the ESR, CRP, RF levels in the moxibustion group and medicine group were significantly decreased ($P < 0.01$), and the level of CRP in the cigarette moxibustion group were significantly decreased ($P < 0.01$). When compared with in the moxibustion group, the levels of ESR, CRP, RF in the cigarette moxibustion group were increased significantly ($P < 0.05$, < 0.01). These results indicated that both moxibustion and

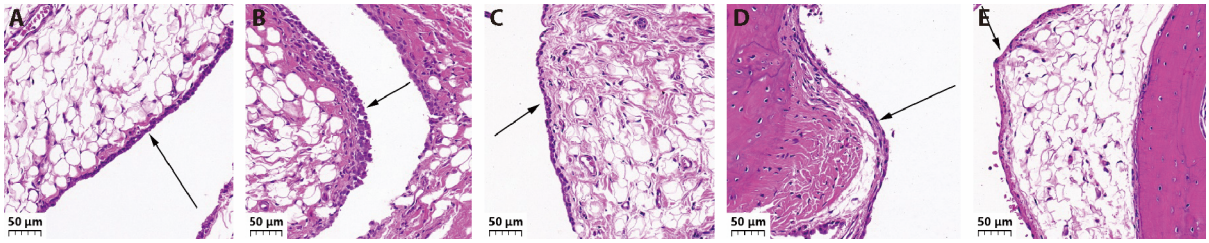

Figure 1 Hematoxylin and eosin staining of the morphology of the synovium of the left hind limb joints of rats
A: normal group; B: model group; C: moxibustion group; D: cigarette moxibustion group; E: medicine group. Normal group were not established of any model or treated with any intervention. Model group were established of rheumatoid arthritis model and treated without any intervention. Moxibustion group were established of rheumatoid arthritis model and treated with moxibustion for 15 d. Cigarette moxibustion group were established of rheumatoid arthritis model and treated with cigarette moxibustion for 15 d. Medicine group were established of rheumatoid arthritis model and treated with tripterygium glycoside (8 mg/kg per day) for 15 d. Black arrow heads synovium. Scale bar = 50 μm.

Tripterygium wilfordii polyglycosides can significantly alleviate RA in rats *via* the influences on specific indicators. And the effects of moxibustion is stronger than those of cigarette moxibustion (Table 2).

3.4. Comparison of the mRNA expression levels of ULK1, autophagy-associated protein (Atg)3, Atg5, and Atg12 in the synovium of the left hind limb joints of rats in each group

When compared with in the normal group, the expression levels of ULK1, Atg3, Atg5, and Atg12 mRNA in the synovium of the left hind limb joints of the model group were significantly decreased ($P < 0.01$), while in the moxibustion group and medicine group were significantly increased ($P < 0.01$). Finally, the relative expression levels of Atg3 and Atg12 mRNA in the cigarette moxibustion group were significantly increased ($P < 0.05$) and the Atg5 and ULK1 mRNA were much significantly increased ($P < 0.01$). When compared with in the moxibustion group, the expression levels of ULK1, Atg3, Atg5, and Atg12 mRNA in the cigarette moxibustion group were decreased significantly ($P < 0.05$), while the ULK1 and Atg3 mRNA in the medicine group were increased significantly ($P < 0.01$); this difference was statistically significant ($P < 0.01$), while the change of Atg5 and Atg12 mRNA was not significant ($P < 0.05$). These results showed that the autophagy of synovium was inhibited in RA model rats and supported that moxibustion and tripterygium glycosides could improve the level of autophagy with an effect that was better than that of cigarette moxibustion (Table 3).

3.5. Expression levels of PI3K, Akt, mTOR, LC3-Ⅱ, and beclin-1 in the synovium of the left hind limb joints of each group

Relative to normal group, the model group increased in the expression levels of PI3K, Akt, mTOR ($P < 0.01$), while the model group decreased in the expression levels of LC3-Ⅱ and beclin-1 ($P < 0.01$). Here, the expression levels of PI3K, Akt, mTOR in the moxibustion group, cigarette group, medicine group decreased ($P < 0.01$), while the expression levels of LC3-Ⅱ and beclin-1 were significantly higher than those of the model group ($P < 0.01$). Meanwhile, the expression levels of PI3K, Akt, and mTOR were lower and the expression levels of LC3-II and beclin-1 were higher in the moxibustion group and medicine group when compared with those in the cigarette group ($P < 0.01$). These results suggest that the PI3K/Akt/mTOR signaling pathway in the synovium of RA rats is active and the autophagy level is decreased. Both moxibustion and tripterygium glycosides can inhibit the PI3K/Akt/mTOR signaling pathway and increase the autophagy level, while the treatment of cigarette moxibustion shows weaker effects (Figure 2).

3.6. Expression levels of p-PI3K, p-Akt, p-mTOR in the synovium of the left hind limb joints of each group

Compare with the normal group, the model group were higher in the expression levels of p-PI3K, p-Akt, p-mTOR ($P < 0.01$). The expression levels of p-PI3K, p-Akt, p-mTOR in the moxibustion group, cigarette group, medicine group decreased than those in the model group ($P < 0.01$). In addition, the expression levels of p-PI3K,

Table 2 Level of ESR, CRP, RF ($\bar{x} \pm s$)

Group	*n*	ESR (mm/h)	CRP (mg/L)	RF (ng/L)
Normal	8	3.3±1.0	4.3±1.6	26.2±6.8
Model	8	10.8±2.7[a]	19.0±2.1[a]	84.1±11.1[a]
Moxibustion	8	7.1±1.9[b]	12.1±2.6[b]	52.5±6.7[b]
Cigarette	8	10.2± 1.7[c]	16.9±2.8[bd]	73.6±8.9[d]
Medicine	8	7.4±1.8[be]	10.5±2.0[bf]	44.1±5.3[bf]

Notes: normal group (Normal) were not established of any model or treated with any intervention. Model group (Model) were established of rheumatoid arthritis model and treated without any intervention. Moxibustion group (Moxibustion) were established of rheumatoid arthritis model and treated with moxibustion for 15 d. Cigarette moxibustion group (Cigarette) were established of rheumatoid arthritis model and treated with cigarette moxibustion for 15 d. Medicine group (Medicine) were established of rheumatoid arthritis model and treated with tripterygium glycoside (8 mg/kg per day) for 15 d. ESR: sedimentation rate; CRP: C-reactive protein; RF: rheumatoid factor. [a]$P < 0.01$, *vs* normal group; [b]$P < 0.01$, *vs* model group; [c]$P < 0.05$ and [d]$P < 0.01$, *vs* moxibustion group; [e]$P < 0.05$ and [f]$P < 0.01$, *vs* cigarette moxibustion group.

Table 3 Gene expression of autophagy process ($\bar{x} \pm s$)

Group	*n*	Atg3 mRNA	Atg5 mRNA	Atg12 mRNA	ULK1 mRNA
Normal	6	1.00±0.03	1.00±0.12	1.00±0.13	1.00±0.05
Model	6	0.35±0.03[a]	0.42±0.04[a]	0.49±0.04[a]	0.32±0.04[a]
Moxibustion	6	0.57±0.05[b]	0.63±0.03[b]	0.72±0.01[b]	0.66±0.04[b]
Cigarette	6	0.42±0.02[bd]	0.52±0.02[c]	0.61±0.03[cb]	0.46±0.03[bd]
Medicine	6	0.79±0.06[bde]	0.73±0.02[be]	0.78±0.02[be]	0.77±0.05[bde]

Notes: normal group (Normal) were not established of any model or treated with any intervention. Model group (Model) were established of rheumatoid arthritis model and treated without any intervention. Moxibustion group (Moxibustion) were established of rheumatoid arthritis model and treated with moxibustion for 15 d. Cigarette moxibustion group (Cigarette) were established of rheumatoid arthritis model and treated with cigarette moxibustion for 15 d. Medicine group (Medicine) were established of rheumatoid arthritis model and treated with tripterygium glycoside (8 mg/kg per day) for 15 d. Atg: autophagy-associated protein; ULK: autophagy-initiating protein kinase; mRNA: messenger ribonucleic acid. [a]$P < 0.01$, *vs* normal group; [b]$P < 0.01$, *vs* model group; [c]$P < 0.05$ and [d]$P < 0.01$, *vs* moxibustion group; [e]$P < 0.01$, *vs* cigarette moxibustion group.

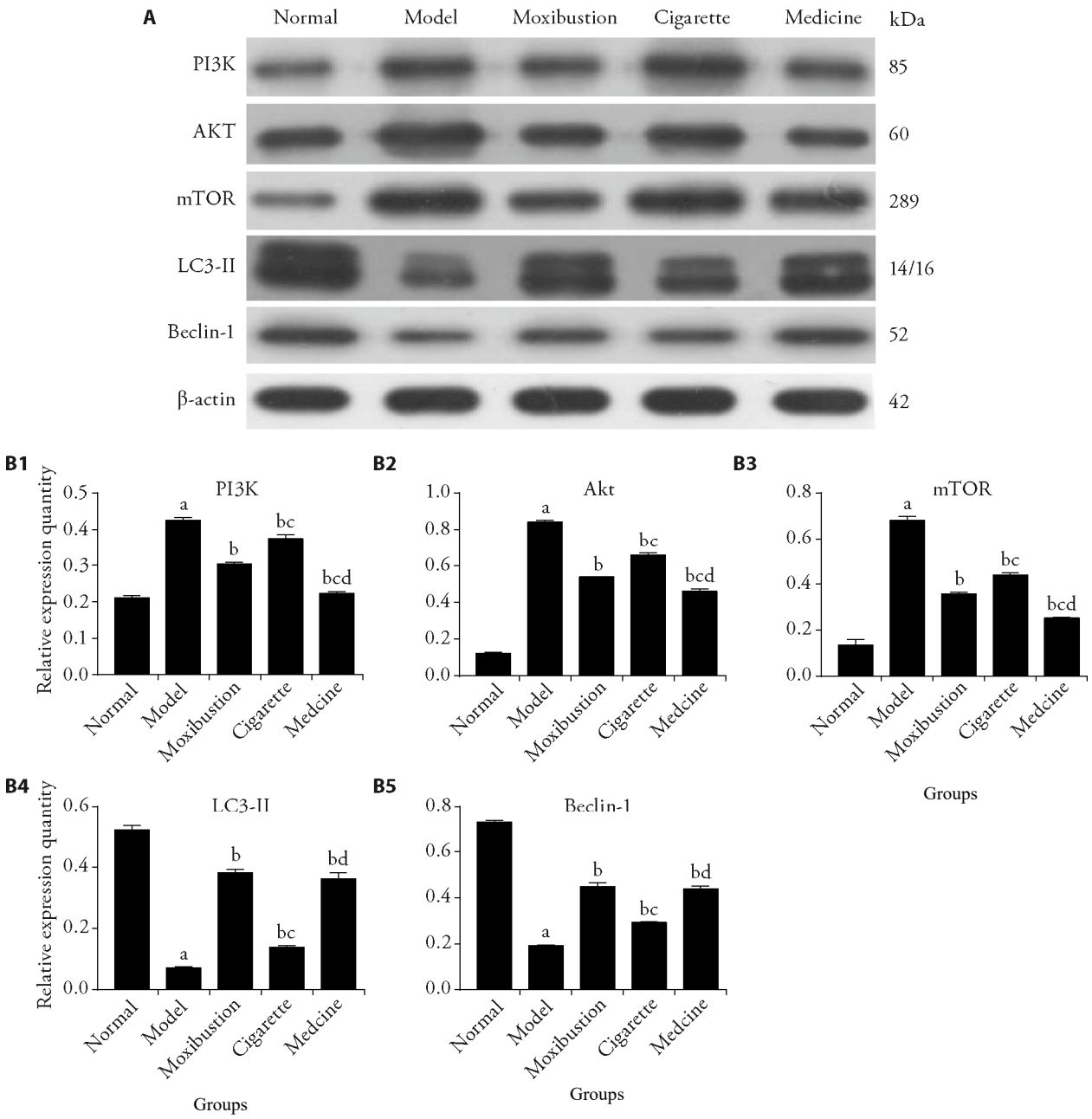

Figure 2 Key protein expression in the autophagy process

A: images of Western blot; B1-B5: relative expression quantity of PI3K, Akt, mTOR, LC3-Ⅱ, Beclin-1. Normal group (Normal) were not established of any model or treated with any intervention. Model group (Model) were established of rheumatoid arthritis model and treated without any intervention. Moxibustion group (Moxibustion) were established of rheumatoid arthritis model and treated with moxibustion for 15 d. Cigarette moxibustion group (Cigarette) were established of rheumatoid arthritis model and treated with cigarette moxibustion for 15 d. Medicine group (Medicine) were established of rheumatoid arthritis model and treated with tripterygium glycoside (8 mg/kg per day) for 15 d. All values are mean ± standard deviation (n = 6). PI3K: phosphatidylinositol-3-kinase; Akt: protein kinase B; mTOR: mammalian target of rapamycin; LC3-Ⅱ: microtubule-associated protein light chain 3-Ⅱ. $^{a}P < 0.01$, *vs* normal group; $^{b}P < 0.01$, *vs* model group; $^{c}P < 0.01$, *vs* moxibustion group; $^{d}P < 0.01$, *vs* cigarette moxibustion group.

p-Akt, and p-mTOR were lower in the moxibustion group and medicine group when compared with those in the cigarette group ($P < 0.01$). These results suggest that the treatments of moxibustion and tripterygium glycosides are able to inhibit the expression of p-PI3K, p-Akt, p-mTOR and increase the autophagy level, while cigarette moxibustion is less effective (Figure 3).

3.7. Comparison of the serum levels of interleukin (IL)-4, IL-6, IL-10, IL-1β, tumor necrosis factor (TNF)-α, IL-23, and IL-17 in the rats of each group

When compared with the normal group, the levels of IL-6, IL-1β, TNF-α, IL-17, and IL-23 in the model group were significantly increased ($P < 0.01$) and the levels of IL-4 and IL-10 were significantly decreased ($P < 0.01$), which indicated that the RA model rats were in an inflammatory reaction state. Compared with in the model group, the levels of IL-6, IL-1β, TNF-α, in the moxibustion group and medicine group were significantly lower ($P < 0.01$) and the levels of IL-4 and IL-10 were significantly higher ($P < 0.01$), IL-17 and

IL-23 in the moxibustion group were significantly lower ($P < 0.01$), while the levels of IL-17 and IL-23 in the medicine group were not significantly lower ($P > 0.05$). IL-6 in the cigarette moxibustion group was higher than in the moxibustion group ($P < 0.01$), IL-1β and IL-23 in the medicine group were higher than in the moxibustion group ($P < 0.05$ or < 0.01), while TNF-α and IL-17 showed no significant difference ($P > 0.05$). IL-6, IL-4, and IL-10 in the medicine group were lower than in the moxibustion group ($P < 0.01$). The levels of IL-6, IL-1β, TNF-α, and IL-23 in the cigarette moxibustion group were higher than those in the moxibustion group ($P < 0.01$), and IL-4, and IL-10 were lower than in the moxibustion group ($P < 0.01$). These results suggest that both moxibustion and medicine treatment can reduce the content of proinflammatory factors and increase the content of anti-inflammatory factors in the serum of experimental RA model rats, although the anti-inflammatory effect of moxibustion is better than that of cigarette moxibustion (Table 4).

4. DISCUSSION

Autophagy is a unique life phenomenon in eukaryotic

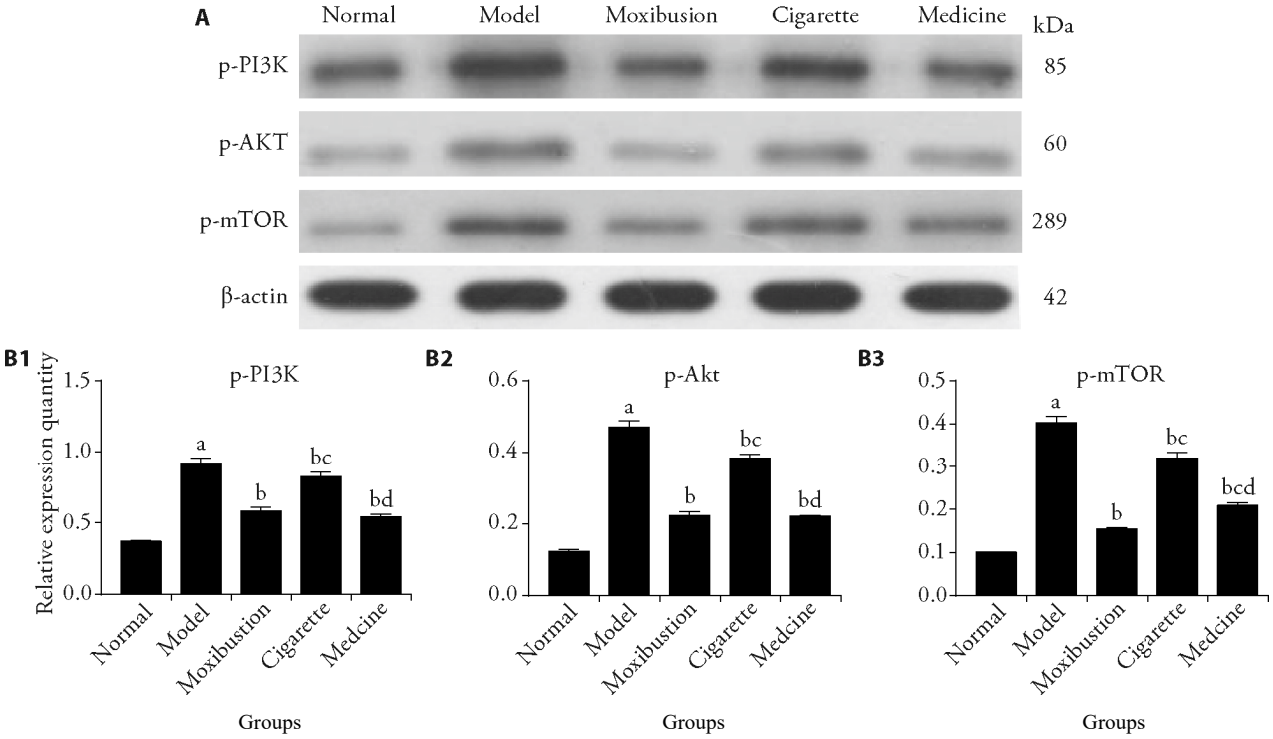

Figure 3 Expression levels of p-PI3K, p-Akt, p-mTOR

A: images of Western blot; B1-B5: relative expression quantity of p-PI3K, p-Akt, p-mTOR. Normal group (Normal) were not established of any model or treated with any intervention. Model group (Model) were established of rheumatoid arthritis model and treated without any intervention. Moxibustion group (Moxibustion) were established of rheumatoid arthritis model and treated with moxibustion for 15 d. Cigarette moxibustion group (Cigarette) were established of rheumatoid arthritis model and treated with cigarette moxibustion for 15 d. Medicine group (Medicine) were established of rheumatoid arthritis model and treated with tripterygium glycoside (8 mg/kg per day) for 15 d. All values are mean ± standard deviation ($n = 6$). p-PI3K: phosphorylated phosphatidylinositol-3-kinase; p-Akt: phosphorylated protein kinase B; p-mTOR: phosphorylated mammalian target of rapamycin. [a]$P < 0.01$, *vs* normal group; [b]$P < 0.01$, *vs* model group; [c]$P < 0.01$, *vs* moxibustion group; [d]$P < 0.01$, *vs* cigarette moxibustion group.

Table 4 Serum levels of IL-4, IL-6, IL-10, IL-1β, TNF-α, IL-23, and IL-17 in rats (pg/mL, $\bar{x} \pm s$)

Group	*n*	IL-1β	IL-6	TNF-α	IL-10	IL-4	IL-17	IL-23
Normal	8	39.4±6.5	4.5±1.0	7.7±1.1	19.6±2.4	55.7±4.5	48.7±5.3	53.4±5.7
Model	8	69.5±7.5	12.9±1.6	14.0±2.4	5.9±1.1	28.5±3.0	68.2±5.8	68.3±4.1
Moxibustion	8	44.0±7.7	7.6±0.9	8.8±1.5	13.3±2.0	45.9±2.7	57.1±8.2	57.1±5.0
Cigarette	8	61.6±6.6	10.8±1.0	12.9±2.2	6.1±1.4	30.0±2.1	62.6±7.5	67.1±3.9
Medicine	8	53.0±6.2	5.8±1.0	8.6±1.2	9.9±1.2	38.7±2.3	63.3±8.7	66.5±4.3

Notes: normal group (Normal) were not established of any model or treated with any intervention. Model group (Model) were established of rheumatoid arthritis model and treated without any intervention. Moxibustion group (Moxibustion) were established of rheumatoid arthritis model and treated with moxibustion for 15 d. Cigarette moxibustion group (Cigarette) were established of rheumatoid arthritis model and treated with cigarette moxibustion for 15 d. Medicine group (Medicine) were established of rheumatoid arthritis model and treated with tripterygium glycoside (8 mg/kg per day) for 15 d. IL: interleukin; TNF: tumor necrosis factor. [a]$P < 0.01$, *vs* normal group; [b]$P < 0.01$, *vs* model group; [c]$P < 0.01$, and [d]$P < 0.05$ *vs* moxibustion group; [e]$P < 0.01$, *vs* cigarette moxibustion group.

cells. The normal process of autophagy is of great significance to the stability of the intracellular environment and the normal progress of cell life activities. It can not only remove abnormal aggregates and damaged organelles in cells but also promote cell senescence and the presentation of cell surface antigens; protect the stability of genomes; and prevent cell necrosis, for which it plays important in waste removal, structural reconstruction, growth and differentiation of cells.[13,14] During the occurrence and development of RA, there are abnormal gene expressions of autophagy and proteins in osteoclasts and synovial fibroblasts.[15,16] Autophagy has two-way regulatory function, which can not only promote cell death under endoplasmic reticulum stress, but also protect synovial cells from apoptosis when proteasome is inhibited.[17,18] On the one hand, autophagy can inhibit the apoptosis of RA synovial cells and protect the cells, but on the other hand, the continuous stimulation of autophagy pathway and the down-regulation of apoptosis will lead to the excessive activation and differentiation of synovial cells, promote the proliferation of synovial cells and aggravate the course of RA.[19, 20]

The process of autophagy is mainly regulated by a series of complexes formed by autophagy-associated protein (Atg), which play an important role in autophagy initiation, the formation of autophagy vesicles, extension, maturation, and degradation. As a homologous protein of Atg1 in mammals, ULK1 has the same function as Atg1.[21, 22] Beclin-1 and microtubule-associated protein light chain 3 (LC3) are homologous genes of Atg6 and Atg8, respectively. They maintain the stability of the internal environment by positively regulating cell autophagy. The levels of beclin-1 and LC3-Ⅱ can monitor the occurrence of autophagy and identify the strength of its activity.[23,24] Atg5 is a key protein involved in the membrane extension of autophagy vesicles that binds Atg12 through a ubiquitin-like reaction; forms a polymer through noncovalent bonds with Atg16; and activates Atg3 enzyme to promote the transformation of LC3 from phosphatidylethanolamine to LC3-Ⅱ-PE, which is closely bound to the surface of autophagy vesicles, and participates in the expansion of preautophagosomes.[25,26] The PI3K/Akt/mTOR signaling pathway is involved in the regulation of autophagy, where PI3K is a heterodimer:[27] here, the subunit p110 binds to Ras and activates PI3K, producing PiP3 and activating the phosphorylated Akt.[28] The activation of PI3K/Akt can further produce mTOR and finally reduce autophagy activity by inhibiting the formation of phagocytic membrane.[29] Studies have shown that the PI3K/Akt/mTOR pathway in the local tissue of an RA joint is activated, which reduces the ability of cells to maintain homeostasis, increases apoptosis, and destroys structure and function; on the contrary, the inhibition of the PI3K/Akt/mTOR pathway can effectively improve the symptoms of RA[30] and can reduce the proliferation of chondrocytes in RA rats, promoting apoptosis and autophagy.[4]

At the early stage of RA, immunocytes are activated to release cytokines such as the IL family and TNF-α.[31,32] TNF-α can provoke the overexpression of bseclin-1; induce the activation of autophagy-related motifs; and promote the monocytes to differentiate into mature osteoclasts and enhance their ability of resorption, resulting in bone resorption at the joint.[33,34] IL-1 maintains chronic inflammation in RA.[33] IL-6 can enhance the proinflammatory effect of cytokines such as IL-1 and TNF- α, induce the production of IL1 and IL-17,[35] and increase the destruction of the joint in patients with RA.[36] IL-23 mediates the production of IL-17 through the STAT3 signal pathway and can enhance and maintain the release of IL-17.[37] IL-17 can mediate the expression of proinflammatory factors such as IL-6, IL-1β, and TNF-α to aggravate the inflammatory reaction; cause edema in joint; promote synovium proliferation; increase the number of osteoclasts; and destroy the bone in the later stage of RA.[38,39] It was found that the production of IL-17 also depended on the PI3K/Akt pathway[40] and the expression levels of IL-23 and IL-17 were positively correlated with the activity of the PI3K/Akt pathway. In RA, the activation of the PI3K/Akt pathway can increase the levels of IL-23 and IL-17 and further aggravate the inflammatory reaction. The inhibition of PI3K/Akt activity can reduce the levels of IL-17 and IL-23, slowing down the inflammatory response.[41, 42] On the contrary, IL-4 and IL-10 can inhibit inflammation. The clinical observation showed that the symptoms of joint pain and swelling in patients with RA were positively correlated with the levels of related proinflammatory cytokines.[43] Increasing the levels of IL-4 and IL-10 in patients with RA and inhibiting the expression levels of IL-1β, IL-6, TNF-α, and other cytokines can reduce the inflammatory reaction and alleviate joint destruction.[44–48]

Moxibustion is available for the treatment of RA and is effective and safe.[49] Recent studies have indicated that the effects of moxibustion mainly include heat, light, and smoke, of which heat is the most important, for activating the heat-sensitive TRPV pathway to produce a series of biological effects.[50] Moxibustion has the effects of anti-inflammation, analgesia, and immunological regulation, which can significantly reduce the inflammatory swelling, increase the threshold of pain, and improve the symptoms of RA.[51,52] This study found that moxibustion at Zusanli (ST36) on the affected side could improve the swelling of the toe joint and inflammatory proliferation of synovial cells in RA model rats; downregulate the levels of ESR, CRF, RF, and pro-inflammatory factors such as IL-1β, IL-6, IL-23, IL-17, and TNF-α; increase the levels of anti-inflammatory factors IL-4 and IL-10. In addition, after moxibustion, the expression levels of ULK1 mRNA, Atg3 mRNA, Atg5 mRNA, Atg12 mRNA, LC3-II, and beclin-1 in the synovium of RA model rats increased significantly, while the expression levels of PI3K, Akt, and mTOR decreased, suggesting that moxibustion can inhibit the PI3K/Akt/mTOR pathway and enhance the level of autophagy of synoviocytes in RA model rats.

In conclusion, in this study, we speculated that moxibustion may enhance the autophagy of synovial cells, inhibit the proliferation of synovial cells, and improve the local inflammatory reaction by reducing the activity of the PI3K/Akt/mTOR pathway such that the disorder of local inflammatory reaction and autophagy of joint can be corrected to a certain extent, alleviating the local symptoms of RA. Our findings help to provide new evidence for the efficacy and mechanism of moxibustion in the treatment of RA. However, due to limited time and financial support, we only discussed the regulatory effect of moxibustion on synovitis and autophagy in RA rats through the PI3K/Akt/mTOR pathway. More research needs to be conducted involving other signaling pathways to further confirm our results.

5. ACKNOWLEDGMENTS

We thank LetPub (www.letpub.com) for its linguistic assistance during the preparation of this manuscript.

6. REFERENCES

1. Seca S, Patrício M, Kirch S, Franconi G, Cabrita AS, Greten HJ. Effectiveness of acupuncture on pain, functional disability, and quality of life in rheumatoid arthritis of the hand: results of a double-blind randomized clinical trial. J Altern Complement Med 2019; 25: 86-97.
2. Shen B, Sun Q, Chen H, et al. Effects of moxibustion on pain behaviors in patients with rheumatoid arthritis: a Meta-analysis. Medicine (Baltimore) 2019; 98: e16413.
3. Zhang W, Chen M, Hu J. Long-snake moxibustion for rheumatoid arthritis: a randomized controlled trial. Zhong Guo Zhen Jiu 2016; 12; 36: 694-8.
4. Feng FB, Qiu HY. Effects of Artesunate on chondrocyte proliferation, apoptosis and autophagy through the PI3K/AKT/mTOR signaling pathway in rat models with rheumatoid arthritis. Biomed Pharmacother 2018; 102: 1209-20.
5. Lin J, He Y, Wang B, et al. Blocking of YY1 reduce neutrophil infiltration by inhibiting IL-8 production *via* the PI3K-Akt-mTOR signaling pathway in rheumatoid arthritis. Clin Exp Immunol 2019; 195: 226-36.
6. Wu X, Long L, Liu J, et al. Gambogic acid suppresses inflammation in rheumatoid arthritis rats *via* PI3K/Akt/mTOR signaling pathway. Mol Med Rep 2017; 16: 7112-8.
7. Dai Y, Hu S. Recent insights into the role of autophagy in the pathogenesis of rheumatoid arthritis. Rheumatology (Oxford). 2016; 55: 403-10.
8. Yuan J, Hu L, Song XG, et al. Influence of moxibustion on TLR 4-MyD 88-NF-KB signal transduction pathway of synovial tissue in rheumatoid arthritis rats. Zhen Ci Yan Jiu 2015; 40: 199-204.
9. Yuan J, Hu L, Song XG, et al. Effect of moxibustion on Toll-like receptor 4-bone marrow differentiation factor 88-nuclear factor kappa B signal pathway in synovial tissue of rats with rheumatoid arthritis. Zhen Ci Yan Jiu 2015; 40: 199-204.
10. Zheng B, Hu L, Song X, et al. Analgesic effect of different moxibustion durations in rheumatoid arthritis rats. J Tradit Chin Med 2014; 34: 90-5.
11. Peng CY, Luo L, Hu L, et al. Effects of different doses of Freund's complete adjuvant on replication in rats with rheumatoid arthritis. Zhong Guo Yi Yao Zhi Nan 2012; 10: 90-5.
12. Lin WZ, Wang P. Experimental acupuncture. First Edition. Shanghai: Shanghai Science and Technology Press, 1999: 277-82.
13. Shahrabi S, Paridar M, Zeinvand-Lorestani M, et al. Autophagy regulation and its role in normal and malignant hematopoiesis. J Cell Physiol 2019; 234: 21746-57.
14. Mizushima N, Komatsu M. Autophagy: renovation of cells and tissues. Cell 2011; 11; 147: 728-41.
15. Manganelli V, Recalchi S, Capozzi A, et al. Autophagy induces protein carbamylation in fibroblast-like synoviocytes from patients with rheumatoid arthritis. Rheumatology (Oxford). 2018; 57: 2032-41.
16. Kato M, Ospelt C, Gay RE, Gay S, Klein K. Dual role of autophagy in stress-induced cell death in rheumatoid arthritis synovial fibroblasts. Arthritis Rheumatol 2014; 66: 40-8.
17. Yin H, Wu H, Chen Y, et al. The therapeutic and pathogenic role of autophagy in autoimmune diseases. Front Immunol 2018; 31; 9: 1512.
18. Qi Z, Chen L. Endoplasmic reticulum stress and autophagy. Adv Exp Med Biol 2019; 1206: 167-77.
19. Xu K, Xu P, Yao JF, Zhang YG, Hou WK, Lu SM. Reduced apoptosis correlates with enhanced autophagy in synovial tissues of rheumatoid arthritis. Inflamm Res 2013; 62: 229-37.
20. Vomero M, Barbati C, Colasanti T, et al. Autophagy and rheumatoid arthritis: current knowledges and future perspectives. Front Immunol 2018; 18; 9: 1577.
21. Chen Y, He J, Tian M, et al. UNC51-like kinase 1, autophagic regulator and cancer therapeutic target. Cell Prolif 2014; 47: 494-505.
22. Park JM, Seo M, Jung CH, et al. ULK1 phosphorylates Ser30 of BECN1 in association with ATG14 to stimulate autophagy induction. Autophagy 2018; 14: 584-97.
23. Wu D, Hao Z, Ren H, Wang G. Loss of VAPB regulates autophagy in a Beclin 1-dependent manner. Neurosci Bull 2018; 34: 1037-46.
24. Hamurcu Z, Delibaşı N, Geçene S, et al. Targeting LC3 and Beclin-1 autophagy genes suppresses proliferation, survival, migration and invasion by inhibition of Cyclin-D1 and uPAR/Integrin β1/ Src signaling in triple negative breast cancer cells. J Cancer Res Clin Oncol 2018; 144: 415-30.
25. Li SP, He JD, Wang Z, et al. miR-30b inhibits autophagy to alleviate hepatic ischemia-reperfusion injury *via* decreasing the Atg12-Atg5 conjugate. World J Gastroenterol 2016; 22: 4501-14.
26. Otomo C, Metlagel Z, Takaesu G, Otomo T. Structure of the human ATG12-ATG5 conjugate required for LC3 lipidation in autophagy. Nat Struct Mol Biol 2013; 20: 59-66.
27. Khan MA, Jain VK, Rizwanullah M, Ahmad J, Jain K. PI3K/AKT/mTOR pathway inhibitors in triple-negative breast cancer: a review on drug discovery and future challenges. Drug Discov Today 2019; 24: 2181-91.
28. Zhang Y, Yan H, Xu Z, Yang B, Luo P, He Q. Molecular basis for class side effects associated with PI3K/AKT/mTOR pathway inhibitors. Expert Opin Drug Metab Toxicol 2019; 15: 767-74.
29. Barra F, Evangelisti G, Ferro Desideri L, et al. Investigational PI3K/AKT/mTOR inhibitors in development for endometrial cancer. Expert Opin Investig Drugs 2019; 28: 131-42.
30. Feng FB, Qiu HY. Effects of Artesunate on chondrocyte proliferation, apoptosis and autophagy through the PI3K/AKT/mTOR signaling pathway in rat models with rheumatoid arthritis. Biomed Pharmacother 2018; 102: 1209-20.
31. Darrieutort-Laffite C, Boutet MA, Chatelais M, et al. IL-1β and TNFα promote monocyte viability through the induction of GM-CSF expression by rheumatoid arthritis synovial fibroblasts. Mediators Inflamm 2014; 2014: 241840.
32. Li Y, Zhang W. IL-6: the next key target for rheumatoid arthritis after TNF-α. Sheng Wu Gong Cheng Xue Bao 2017; 25; 33: 36-43.
33. Lin NY, Beyer C, Giessl A, et al. Autophagy regulates TNFα-mediated joint destruction in experimental arthritis. Ann Rheum Dis 2013; 72: 761-8.
34. Hashizume M, Hayakawa N, Mihara M. IL-6 trans-signalling directly induces RANKL on fibroblast-like synovial cells and is involved in RANKL induction by TNF-alpha and IL-17. Rheumatology (Oxford) 2008; 47(11): 1635-40.
35. Connor AM, Mahomed N, Gandhi R, Keystone EC, Berger SA. TNFα modulates protein degradation pathways in rheumatoid arthritis synovial fibroblasts. Arthritis Res Ther 2012; 14; 14: R62.
36. Fujimoto M, Serada S, Mihara M, et al. Interleukin-6 blockade

suppresses autoimmune arthritis in mice by the inhibition of inflammatory Th17 responses. Arthritis Rheum 2008; 58: 3710-9.
37. Yuan N, Yu G, Liu D, Wang X, Zhao L. An emerging role of interleukin-23 in rheumatoid arthritis. Immunopharm Immunot 2019; 41: 185-91.
38. Kamel KM, Gad AM, Mansour SM, Safar MM, Fawzy HM. Novel anti-arthritic mechanisms of polydatin in complete Freund's adjuvant-induced arthritis in rats: involvement of IL-6, STAT-3, IL-17, and NF-κB. Inflammation 2018; 41: 1974-86.
39. Funaki Y, Hasegawa Y, Okazaki R, et al. Resolvin E1 inhibits osteoclastogenesis and bone resorption by suppressing IL-17-induced RANKL expression in osteoblasts and RANKL-induced osteoclast differentiation. Yonago Acta Med 2018; 28; 61: 8-18.
40. Wei L, Xiong H, Li W, Li B, Cheng Y. Upregulation of IL-6 expression in human salivary gland cell line by IL-17 *via* activation of p38 MAPK, ERK, PI3K/Akt, and NF-κB pathways. J Oral Pathol Med 2018; 47: 847-55.
41. Li H, Min J, Mao X, Wang X, Yang Y, Chen Y. Edaravone ameliorates experimental autoimmune thyroiditis in rats through HO-1-dependent STAT3/PI3K/Akt pathway. Am J Transl Res 2018; 10: 2037-46.
42. Xiao Y, Shi M, Qiu Q, et al. Piperlongumine suppresses dendritic cell maturation by reducing production of reactive oxygen species and has therapeutic potential for rheumatoid arthritis. J Immunol 2016; 15; 196: 4925-34.
43. Chen KH, Li RB, Li K, et al. Clinical effects of moxibustion treatment of rheumatoid arthritis and a study of its blood IL-6 and CRP levels. Zhong Yao Yao Li Yu Lin Chuang 2015; 31: 303-4.
44. Ouyang BS, Che JL, Gao J, et al. Effects of electroacupuncture and simple acupuncture on changes of IL-1, IL-4, IL-6 and IL-10 in peripheral blood and joint fluid in patients with rheumatoid arthritis. Zhong Guo Zhen Jiu 2010; 30: 840-4.
45. Verhoef CM, Van Roon JA, Vianen ME, Bijlsma JW, Lafeber FP. Interleukin 10 (IL-10), not IL-4 or interferon-gamma production, correlates with progression of joint destruction in rheumatoid arthritis. J Rheumatol 2001; 28: 1960-6.
46. Hong H, Zeng Y, Jian W, et al. CDK7 inhibition suppresses rheumatoid arthritis inflammatio *via* blockage of NF-κB activation and IL-1β/IL-6 secretion. J Cell Mol Med 2018; 22: 1292-301.
47. Ogata A, Kato Y, Higa S, Yoshizaki K. IL-6 inhibitor for the treatment of rheumatoid arthritis: a comprehensive review. Mod Rheumatol 2019; 29: 258-67.
48. Nguyen MVC, Baillet A, Romand X, et al. Prealbumin, platelet factor 4 and S100A12 combination at baseline predicts good response to TNF alpha inhibitors in rheumatoid arthritis. Joint Bone Spine 2019; 86: 195-201.
49. Wu X, Zhang Y, Chen B, Luo J, Gan L, Chen G. Moxibustion for rheumatoid arthritis: protocol for a systematic review. Medicine (Baltimore) 2019; 98: e15899.
50. Jiang J, Wang X, Wu X, Yu Z. Analysis of factors influencing moxibustion efficacy by affecting heat-activated transient receptor potential vanilloid channels. J Tradit Chin Med 2016; 36: 255-60.
51. Zhang H, Ma XP, Wu HG, et al. Effect of moxibustion on tumor necrosis factor-α and nuclear transcription factor kappa B in ankle joints of rats with rheumatoid arthritis. J Acupunct Tuina Sci 2017; 15: 171-6.
52. Luo L, Hu L, Song XG, et al. Effect of moxibustion on th emetatarsal joint cytokine in rheumatoid arthritis rats. Huan Qiu Zhong Yi Yao 2011; 4: 416-9.